Appendix 2

THE MEASUREMENT OF RECRYSTALLIZATION

In this appendix we provide a brief overview of some quantitative aspects of recrystallization, including the experimental techniques used to measure recrystallization, the determination of some of the parameters associated with the annealing processes, and the quantification of some important features of the associated microstructures. We do not attempt to cover the subject matter in detail, but aim to highlight important and new aspects of the subject and indicate key references where further information may be obtained. Because the use of EBSD for quantitative metallography is relatively new, the use of this technique will be covered in rather more detail than other methods. As will be discussed below, EBSD enables important microstructural parameters which were hitherto unobtainable, to be determined.

A2.1 TECHNIQUES FOR MEASURING RECRYSTALLIZATION

Recrystallization and the other annealing phenomena discussed in this book are all processes of microstructural evolution, and most techniques available for studying the microstructure of crystalline materials may be used to measure some aspect of recrystallization. Brief comments on the main techniques which have been employed are given below, and some further details of their applications in specific areas are given in subsequent sections.

A2.1.1 Optical microscopy

As the earliest metallographic technique, optical microscopy is too well known to require further explanation here. With a spatial resolution of ~0.5 μm, it is frequently used for both opaque and transparent materials and has the advantages that it is simple, rapid and inexpensive and can be used to examine large areas. Because of this, it should always be the first method employed to examine an annealed material. However, the amount and accuracy of the information which may be obtained is often limited by the contrast mechanism employed (e.g. surface contrast from etching or contrast from anodic films, and in many cases only partial microstructural information is obtainable.

A2.1.2 Transmission electron microscopy (TEM)

Diffraction contrast in the TEM allows the study of individual dislocations at a spatial resolution of ~5 nm, and the evolution of dislocation structures during recovery. Quantitative measurements of dislocation densities and particle content can be made, although their accuracy depends critically on measurement of the thickness of the thin foil specimens. Recovery, and the early stages of recrystallization may be studied, although the limited area of the sample makes quantitative analysis difficult. In-situ annealing experiments (e.g. fig. 9.10) provide some clues as to the nature of the annealing processes, but the strong effects of the surfaces in samples which are often less than 1 μm thick, may lead to microstructural changes which would not occur in bulk samples.

A2.1.3 Scanning electron microscopy (SEM)

Although the SEM may be used on etched samples as a 'high resolution optical microscope', its main advantage is the availability of diffraction or 'channelling' contrast when using backscattered electrons. This is a similar contrast mechanism to that of the TEM, and although individual dislocations cannot generally be detected (Wilkinson and Hirsch 1997), small changes in orientation across low angle boundaries enable them to be readily imaged (e.g. fig. 7.1). With a FEGSEM operating at ~10 keV, substructures can be revealed with a spatial resolution of ~25 nm in aluminium, and even better resolution is obtainable in heavier metals. As the sample is only polished on one surface, large areas may be examined, and the technique is ideal for measuring the progress of recrystallization and the determination of grain and subgrain sizes. In-situ annealing experiments in the SEM are readily undertaken, and provide valuable information (e.g. fig. 7.2). The presence of only one free surface makes such experiments more reliable than those carried out in the TEM, although great caution must still be used in their interpretation.

A2.1.4 Electron backscatter diffraction (EBSD)

The principles of EBSD are discussed in appendix 1, with particular relevance to the determination of textures. However, the use of EBSD as a technique for quantitative

metallography is now widely recognised, and is discussed by Humphreys (2001). Using EBSD maps, both the size and orientation of grains and subgrains may be determined, and detailed metallography of partly recrystallized samples carried out. The current limitations of the technique for studying deformed materials are primarily the spatial and angular resolutions (see table A1.2). Nevertheless, even highly deformed samples of a subgrain-forming material such as aluminium may be successfully studied as shown in figure 14.4.

A2.1.5 X-ray diffraction

In addition to its use for texture determination, x-ray diffraction may be used to investigate the deformed state and the annealing of materials in a number of ways including stored energy measurement. (§A2.2.1), and boundary migration during grain growth (§A2.7.2). Changes in texture during dynamic heating experiments may be followed by x-ray or neutron diffraction (Hansen et al. 1981), and with care, interpreted in terms of microstructural evolution. There is currently an interest in developing x-ray microscopy based on synchrotron radiation for investigating recrystallization and grain growth (Juul Jensen and Poulson 2000). This would have the benefits of providing 3-D information and enabling 3-D in situ annealing experiments to be carried out. However, it is too early to ascertain if sufficient spatial resolution will be obtainable by this technique for the measurement of recrystallization.

A2.1.6 Ultrasonics

A relatively new technique for studying microstructure, which is particularly suitable for dynamic measurements is laser-ultrasonics (Lindh–Ulmgren et al. 2001). Laser light is pulsed onto the surface of a sample, where it generates an ultrasonic signal. The signal is complex, and may be analysed to reveal changes in elastic modulus, which are related to texture, and also grain structure. As the technique can readily be applied to hot samples and is remote and non-intrusive, it offers the potential for directly monitoring the progress of recrystallization.

A2.1.7 Property measurements

Changes in microstructure during annealing are often reflected in changes in the mechanical properties, and changes in hardness or yield stress can be used to follow recovery or recrystallization (e.g. figs. 6.3–6.6). However, because of the complex relationships between strength and microstructure it is often difficult to unambiguously interpret mechanical property changes in terms of microstructural events.

Physical properties, such as resistivity or density are strongly dependent on defect content, and may be used to follow annealing (e.g. fig. 6.3). However, detailed interpretation of the data in terms of microstructural changes is again difficult.

A2.2 DRIVING PRESSURE FOR RECRYSTALLIZATION

The driving pressure for recrystallization arises from the crystal defects stored in the deformed material. These include high angle grain boundaries, dislocations and dislocation boundaries such as cell or subgrain walls. Unfortunately, this important parameter is very difficult to measure accurately. Brief reviews of methods of measuring the stored energy of deformed metals are given by Borbely and Driver (2001) and Bacroix et al. (2000).

A2.2.1 Calorimetry

A sensitive calorimeter may be used to determine the release of stored energy (Schmidt 1989, Haessner 1990, Scholz et al. 1999), and some of the measurements are discussed in §2.2.2.

However, because of the small amount of stored energy in a deformed material, reliable calorimetric measurements of recovery and recrystallization can only be made on materials in which no phase transformations such as precipitation (e.g.Verdier et al. 1997) or surface reaction (Scholz et al. 1999) occur over the temperature range of the experiment. For example, the stored energy of deformed aluminium is ~20 J/mol (§2.2), and the latent heat released by precipitating a volume fraction of only 0.01 of $CuAl_2$ in aluminium is also ~20 J/mol. It is now thought that some early measurements of stored energy are unreliable because of the occurrence of small amounts of phase transformation during the experiments.

A2.2.2 X-ray diffraction

The lattice distortions due to dislocations can be detected as a broadening of x-ray diffraction peaks, and this has been used to measure stored energies for many years (§2.2). The shape and symmetry of the peaks depend on a number of factors including the overall dislocation density, the long-range stress fields, cell size and grain orientation effects. By measuring the profiles of several diffraction peaks, it is possible to deconvolute the data so as to determine the dislocation arrangements in some detail, and many models for this have been proposed (e.g. Williamson and Hall 1953, Wilkens 1965, Groma et al. 1988). The stored energies of grains of different orientations may be estimated (e.g. fig. 2.7) and the edge or screw character of the dislocations determined (Schaffler et al. 2001).

The use of high intensity x-ray synchrotron sources enables very small volumes containing a few or even single small grains to be investigated, and the high beam intensity and resolution enables further parameters such as cell misorientations to be measured (Borbely and Driver 2001, Bacroix et al. 2000).

A2.2.3 Electron microscopy and diffraction

The stored energy may also be determined from microstructural measurements, the method depending on the dislocation distribution, and we consider three cases.

The dislocations are relatively **uniformly distributed.** In this situation, which is rather unusual (e.g. Al–5%Mg), the stored energy may be estimated from a measurement by TEM of the dislocation density. The stored energy is then calculated from relationships such as equation 2.4.

Well-defined subgrains are formed (e.g. recovered aluminium or metals deformed at high temperatures). In this case, measurements of subgrain size (D) and subgrain misorientation (θ) are best made by EBSD. A relationship between boundary misorientation and boundary energy such as the Read–Shockley relationship of equation 4.5 must be assumed, and the stored energy is then calculated from D and θ, using equations 2.7 or 2.8. However, boundary energies are not well known, and the accuracy and general applicability of equation 4.5 is not well established. In some cases both a subgrain structure and unbound dislocations are formed (§13.2.3), and these terms must both be included.

A **dislocation cell structure** is formed (e.g. deformed copper). This is a very difficult case because the high dislocation density in the cell walls is difficult to measure and the dislocation density is inhomogeneous, making the application of equation 2.4 doubtful.

More detailed reviews of measurements of stored energy by TEM are given by Bacroix et al. (2000) and Borbely and Driver (2001). If the defect structure is more complex, such as in a material which undergoes both slip and deformation twinning (e.g. α-brass or magnesium) there are no established methods for estimating the stored energy from microscopic measurements.

A2.3 FRACTION RECRYSTALLIZED

Measurement of the amount of recrystallization is an essential part of the determination of recrystallization kinetics. Although some indication of this parameter may be obtained from indirect measurements of e.g. hardness or resistivity (e.g. fig. 7.18), accurate measurements can only be obtained by studying the microstructure.

A2.3.1 Microscopical methods

Optical microscopy is traditionally used to measure the progress of recrystallization, and similar results may be obtained by SEM imaging. If the recrystallized and unrecrystallized regions can be distinguished by e.g. etching, then standard methods of quantitative metallography using areal, lineal or point counting methods may be employed (Orsetti Rossi and Sellars 1997). Point counting is the most efficient, and this may be carried out using a standard point-counting microscope. If $\mathbf{n_r}$ is the number of the measured points which are recrystallized in a sample whose recrystallized fraction is $\mathbf{X_V}$, the confidence limits (σ) are given (Gladman and Woodhead 1960) as

$$\left(\frac{\sigma}{X_V}\right)^2 = \frac{1 - X_V}{n_r} \tag{A2.1}$$

For a sample which is ~50% recrystallized, the number of measurements required is typically ~500, but for $X_V < 0.1$ the number of points required is unrealistically large for such a manual technique (Orsetti Rossi and Sellars 1997).

A2.3.2 EBSD methods

There are several ways in which EBSD may be used to determine the fraction recrystallized (Humphreys 2001).

- **Point counting**

If it is possible to distinguish between the diffraction patterns from recrystallized and unrecrystallized material, then point counting methods may be used. Such techniques rely on the quality of the diffraction pattern being lower in an unrecrystallized region than in a recrystallized grain due to dislocation debris. Several approaches have been proposed (e.g. Black and Higginson 1999, Tarasiuk et al. 2001), but although such methods are very rapid, careful calibration is required. In most aluminium alloys deformed at room temperature and many metals deformed at elevated temperatures, the subgrain structures are relatively clean, and of an area larger than the EBSD resolution (table A1.2). Therefore the diffraction patterns obtained from within subgrains in the deformed regions will be of similar quality to those for recrystallized regions, and in this case, point counting techniques based on pattern quality do not work reliably.

- **Lineal analysis**

In a subgrain-forming material (e.g. aluminium), lineal EBSD analysis may be used. One method is to identify high or low angle boundaries during a scan and to assume that the region between two adjacent boundaries which are high angle, is a recrystallized grain (Humphreys 2001). Alternatively, the fraction of boundaries which are high angle can be measured from a linescan, and this provides an indirect measure of the fraction recrystallized (see fig. 14.6).

- **Areal analysis**

The fraction recrystallized may be obtained from analysis of EBSD maps (Humphreys 2001). Although the technique is considerably slower than point counting methods, it is particularly suitable for studying the early stages of recrystallization, and can be used to identify the orientation distributions of the recrystallizing grains. The recrystallized regions may be identified on the basis of pre-defined size, pattern quality, size and boundary character criteria, and although very detailed measurements may be made in this way, there are rather few cases when such a time-consuming method is justified.

A2.4 NUCLEATION AND GROWTH RATES

The overall rate of recrystallization during isothermal annealing may be found from the increase in the volume recrystallized (§A2.3) as a function of time. However, a more detailed interpretation of the recrystallization behaviour is often obtained by determining the rates of nucleation and growth of the new grains. Recent reviews include those of Orsetti Rossi and Sellars (1997) and Juul Jensen (2001).

A2.4.1 Nucleation of recrystallization

The nucleation of recrystallization is discussed in chapter 7, where it was pointed out that the rate of nucleation (dN/dt) was a complex parameter. For simplicity, two

possibilities are usually considered, **site-saturated nucleation,** where all nuclei are present at $t = 0$ or a **constant nucleation rate.**

The most common method of distinguishing between these possibilities is by counting the grains per unit area (N_p) on a 2-D section from microscopic or EBSD data, and using standard quantitative metallographic analyses (e.g. Fullman 1953). As the nuclei grow, then N_p increases, and if it is assumed that the nuclei are spheres of radius **r,** the number of nuclei per unit volume (N) is given by

$$N = \frac{N_p}{2r} \tag{A2.2}$$

This analysis can be extended to allow for nuclei of different sizes and shapes (Fullman 1953).

Alternatively, the microstructural path analysis of Vandermeer and Rath (1989a) based on the work of Gokhale and DeHoff (1985), which is discussed in §7.3.2 may be used. This is based on the variation with time of the extended recrystallized volume fraction (X_{VEX}) and extended interfacial area per unit volume between recrystallized and unrecrystallized material (S_{VEX}), which are given by equations 7.25 and 7.26 respectively. From the term δ, obtained via equation 7.30 from the exponents **n** and **m** in these equations, it is possible to determine the type of nucleation. If $\delta = 0$ then nucleation is site saturated and if $\delta = 1$ then the nucleation rate is constant. The analysis is strictly valid only for a random spatial distribution of nuclei, although it can be modified to allow for non-random distributions (see e.g. Orsetti Rossi and Sellars 1997).

A2.4.2 Growth rates

The simplest method of determining the growth rates of recrystallizing grains is to measure the sizes of the largest grains visible on 2-D sections as a function of annealing time (Anderson and Mehl 1945). However, this method is only applicable in the early stages of recrystallization, before impingement of the grains occurs.

A better method of measuring growth rates is that suggested by Cahn and Hagel (1960) and given by equation 7.18. This requires measurement from 2-D sections of the fraction recrystallized ($\mathbf{X_V}$) and the area per unit volume between recrystallized and unrecrystallized material ($\mathbf{S_V}$). Both these parameters can be readily measured by standard microscopical methods or by EBSD. From EBSD data, it is possible to extend this analysis to measure the growth rates of recrystallizing grains of particular orientations (e.g. Juul Jensen 1995a). More detailed information as to whether growth rates are anisotropic may be obtained from methods such as those proposed by Vandermeer and Rath (1989a), and outlined in §7.3.2.

A2.5 GRAIN AND SUBGRAIN SIZE

The grain size has traditionally been measured by optical microscopy, and the methods of determining grain size and related parameters have been well

documented (e.g. DeHoff and Rhines 1968, Underwood 1970. Scanning electron microscopy is increasingly being used, although, as with any scanning technique, particular care must be taken with instrument calibration (Dyson and Quested 2001). For the smallest grain sizes and for subgrain structures, transmission electron microscopy (TEM) may be required, although the problems of preparing and working with the thin specimens required for TEM make it difficult to measure representative microstructures, and the subtleties of the image contrast make automated analysis of TEM images very difficult. EBSD is increasingly being used to characterise grain and subgrain structures, and this has the additional advantage that dimensional information may readily be correlated with the grain or subgrain orientations (Humphreys 2001). Because the sample is typically tilted by 70° to the optic axis, great care must be taken with calibration and sample alignment if accurate measurements are required.

A2.5.1 EBSD measurements

The grain or subgrain size may be determined by EBSD using rather similar methods to those developed for microscopy (Humphreys 2001), and the recent improvements in the speed of EBSD pattern acquisition (table A1.2) enable sufficient data to be obtained in reasonable times.

A significant advantage of EBSD determination over microscopic methods is that EBSD determines all boundaries (above the noise level), whereas metallographic methods only reveal some of the boundaries. Thus optical etching may not reveal low-Σ boundaries or low angle boundaries, and SEM channelling contrast images will only reveal boundaries if the backscattered electron intensity differs between the adjacent grains. Comparison between grain sizes determined by optical imaging, SEM imaging and EBSD (Humphreys 2001), shows significant differences, particularly in recrystallized material with a strong texture.

EBSD **linescans** may be used to obtain values of the mean linear intercept (MLI). By noting orientation changes between successive measurements, the intercept size can be determined for high angle or low angle boundaries, or for any specified angular range. In order to avoid oversampling, the spacing between successive linescans should not be significantly less than the grain/subgrain size. Linear intercepts may either be obtained directly from linescans or from subsequent analysis of an EBSD map, the formed being much faster. The method of determining MLI from analysis of a linescan is given in §A2.5.2.1.

If an EBSD map is obtained, the grains or subgrains may be **reconstructed** by identifying areas whose pixels have orientations within a specified range. This is equivalent to the image analysis methods used for reconstructing metallographic images, and has the advantage that complete information on size, area and shape is obtained. The grain or subgrain size is subsequently determined as an equivalent circle diameter (ECD) as discussed in §A2.5.2.2. The real power of this method is that it enables a significant amount of extra information to be obtained such as the misorientations of all the boundaries of a subgrain and the size and misorientation of subgrains of specific orientations (Humphreys 2001).

When using either linear intercepts or grain reconstruction methods, the size of the steps between adjacent data points is important, because if the step size is too large, small grains or intercepts will be missed and the measured grain/subgrain size will be too large. For an accuracy of ~5%, approximately 10 pixels per grain/subgrain are required (Humphreys 2001). For small grain or subgrain sizes, the EBSD pattern solving efficiency is reduced (A1.3.4.1), and it has been shown that when less than ~50% of patterns are solved, significant errors in the size measurements occur (Humphreys 2001). The step size and pattern solving factors therefore set a lower limit on the grain or subgrain size which can accurately be measured by EBSD, and for aluminium, these are currently ~0.15 μm and 0.4 μm for FEGSEM and W-filament microscopes respectively (Humphreys 2001).

A2.5.2 Calculation of size

If intercept or area measurements of grains or subgrains are made, the following analyses, based on the work of Fullman (1953) and Underwood (1970) may be used to obtain the grain sizes.

A2.5.2.1 Mean linear intercept

For a single-phase material of uniform grain size the grain size may be related to $\overline{L}$, the mean linear intercept distance (MLI) across a grain as measured on a plane section. $\overline{L}$ is determined by measuring the average number of boundary intercepts (N_L) with a line of unit length so that

$$\overline{L} = 1/N_L \tag{A2.3}$$

The boundary surface area per unit volume (S_V) is given by

$$SV = 2N_L \tag{A2.4}$$

$\overline{L}$ will be less than the true grain size because of sectioning effects. If it is assumed that the grain shapes approximate to spheres of diameter $\overline{D}$ then

$$\overline{D} = 1.5\overline{L} \tag{A2.5}$$

$\overline{L}$ is a simple unambiguous parameter which is often used to characterise a grain structure. If the grains are not equiaxed then they can be characterised by mean linear intercepts in the x, y and z directions. However, these cannot readily be converted to a mean diameter.

A2.5.2.2 Equivalent circle diameter

If spherical grains of diameter $\overline{D}$ intersect a random plane, the mean area of intersection is

$$\overline{S} = \pi D^2/6 \tag{A2.6}$$

If these areas are circular, the mean diameter is the **Equivalent Circle Diameter** (ECD) which is given by

$$\mathrm{ECD} = (2/3)^{1/2}\overline{D} = 0.816\overline{D} \tag{A2.7}$$

Note that the ECD is not the same as the MLI, and for uniform spherical grains

$$\mathrm{ECD} = 1.224\overline{L} \tag{A2.8}$$

If the grains are not equiaxed, an ECD is less valid and alternative parameters such as the mean grain area $\overline{S}$ or the mean grain dimensions in orthogonal directions can be used.

A2.5.3 Precision of measurement

If the data set comprises N measurements (e.g. intersections) of a parameter X, then the **mean is** $\mathrm{X} = \sum \mathrm{X_i}/\mathrm{n}$. The **standard deviation** (σ) is

$$\sigma = \sqrt{\frac{(\mathrm{X_i} - \overline{\mathrm{X}})^2}{\mathrm{n}-1}} = \sqrt{\frac{\mathrm{X_i^2} - (\mathrm{X_i})^2/\mathrm{n}}{\mathrm{n}-1}} \tag{A2.9}$$

The standard error of the mean (SE) is

$$\mathrm{SE} = \frac{\sigma}{\sqrt{\mathrm{n}}} = \sqrt{\frac{(\mathrm{X} - \overline{\mathrm{X}})^2}{\mathrm{n}(\mathrm{n}-1)}} \tag{A2.10}$$

The 95% confidence limit is $\overline{\mathrm{X}} \pm 2\,\mathrm{SE}$, and it is recommended that grain/subgrain sizes are presented in this form.

It is usually found that ~300–400 grain or intersection measurements are required to give sufficient precision.

A2.6 GRAIN BOUNDARY CHARACTER DISTRIBUTION

The development of EBSD has made the characterisation of grain boundary misorientations relatively simple, and parameters such as the distribution of grain boundary character (GBCD) in a sample may be rapidly obtained. The three parameters which are of particular significance are the **angle** and **axis** of misorientation and the **boundary plane.**

A2.6.1 Misorientation angle

The misorientation distribution, which was first discussed by McKenzie (1958), is shown for an ideal random polycrystalline assembly in figure 4.2. However, it is sensitive to the

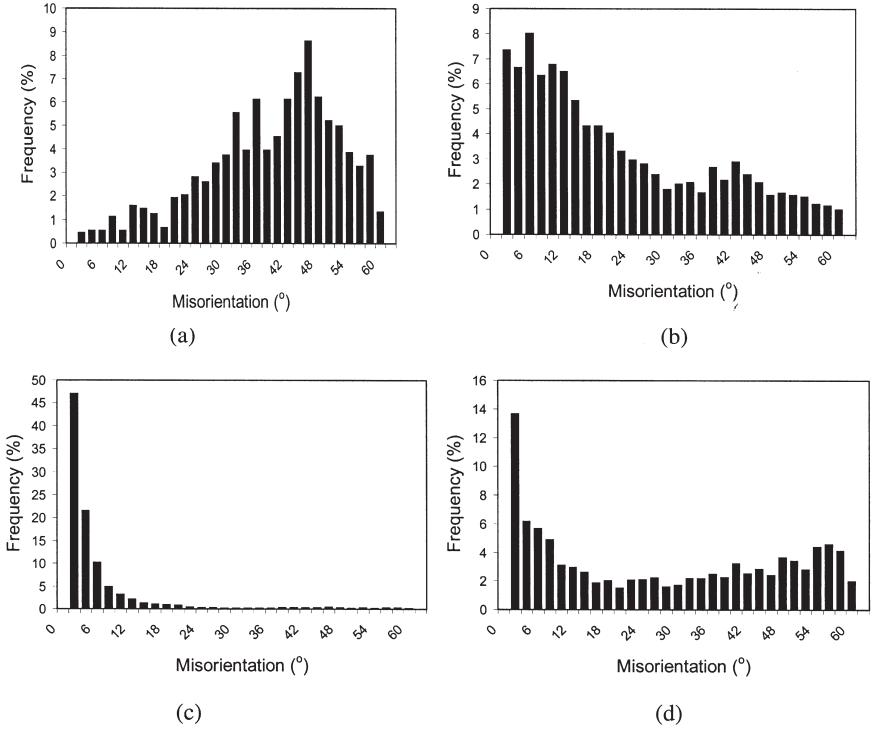

Fig. A2.1. Examples of grain boundary misorientation distributions (McKenzie plots), obtained by EBSD, in commercial purity aluminium. (a) Recrystallized, with random texture, showing a distribution close to that of figure 4.2. (mean misorientation 39.6°, %HAGB = 95), (b) Recrystallized to strong cube texture (mean misorientation 21.9°, %HAGB = 55), (c) Cold rolled 20% (mean misorientation 7.4°, %HAGB = 9.8), (d) Cold rolled 98% (mean misorientation 28°, %HAGB = 63).

texture of the material, and is also altered by plastic deformation and annealing, and examples are shown in figure A2.1. Subsets of the data such as the fraction of high angle and low angle boundaries (e.g. fig. 14.6) or the fractions of low-Σ boundaries, are now becoming commonly used parameters of a thermomechanically processed material and many examples are given in this book.

The frequencies of boundaries of particular types may be obtained as **length** fractions or **number** fractions depending on the method of data analysis (Humphreys 2001). The data are normally obtained from measuring the misorientations of adjacent grains, but the **uncorrelated misorientation distribution** (e.g. table 2.7), can also be determined by comparing the misorientations between all pixels or subgrains in a measured area. This parameter gives a measure of the orientation spread within the area and is thus an indication of long range orientation gradients.

The accuracy of the misorientation data are limited by the precision with which the diffraction patterns are analysed. In high speed EBSD acquisition, which is normally

used for microstructural investigations (table A1.2), the misorientations are typically accurate to within $\sim 1^\circ$, although this may be considerably reduced by data averaging and filtering (Humphreys et al. 2001a). The relative angular resolution may be improved by a factor of up to ~ 10 if techniques involving direct comparison of successive diffraction patterns are used (e.g. Wilkinson 2001). However, such procedures are comparatively slow and are not yet widely used.

A2.6.2 Misorientation axis

In addition to the angles, the axes of misorientation and their distributions may also be of interest, and these are readily obtained when the misorientations are determined. The errors in determining the angle of misorientation limit the accuracy with which the misorientation axis can be determined, and this is particularly important for small misorientations (Prior 1999, Wilkinson 2001).

A2.6.3 Boundary plane

The two degrees of freedom describing the boundary plane are less readily determined experimentally. Trace analysis has long been used to obtain partial information, and when combined with EBSD, this enables one of the boundary plane parameters to be determined. The other parameter, which is the inclination of the boundary to the surface of the sample, is not directly obtainable, and is discussed by Randle and Engler (2000). For large grains, the boundary plane may be determined by sectioning and examining the sample in two orthogonal planes, or in the more general case, by serial sectioning in which the sample is measured after controlled etching.

A2.7 GRAIN BOUNDARY PROPERTIES

The energies and mobilities of boundaries are important during recovery, recrystallization and grain growth. However, measurements of both parameters are very difficult, and additionally there are a large number of important variables including the 5 grain boundary degrees of freedom (§4.1), and the effects of solute, temperature and driving pressure. It is therefore not surprising that a coherent and comprehensive picture of grain boundary properties has not yet been obtained.

A2.7.1 Boundary energy

Measurement of the absolute energies of boundaries is difficult and in most cases the measurements are made relative to a reference interface or surface (see e.g. Hondros 1969, Gottstein and Shvindlerman 1999). If torque terms can be neglected, the geometry of a triple point or groove is given by equation 4.10, and the results shown in figure 4.12 were obtained in this manner. In a variation on this method, the equilibrium shapes of amorphous silica particles at grain boundaries in copper are measured (Mori et al. 1988,

Goukon et al. 2000). This method is very sensitive and avoids the inevitable problems associated with tri-crystals or grooving experiments at free surfaces.

In a novel large-scale investigation of boundary properties, Rollett and colleagues (e.g. Yang et al. 2001) have determined the boundary properties of aluminium from detailed measurements of triple junctions in thick foils. The boundary geometry is simplified by the columnar grain structure which develops in the foils. If it is assumed that the migration rate is proportional to the driving pressure which arises from capillarity (equation 7.1) it is possible from detailed measurements of triple point angles, boundary shapes and grain orientations, together with detailed theoretical analysis, to ascertain boundary energies and mobilities. The measurements of the effect of misorientation on boundary energy are in good agreement with the Read–Shockley relationship of equation 4.5, although a small effect of the misorientation axis is found (fig. 4.7).

A2.7.2 Boundary mobility

Information about boundary mobilities may be made from measurements of individual boundaries or from the growth of a subgrain or grain assembly. Reviews of the techniques used are given by Gleiter and Chalmers (1972), Masteller and Bauer (1978) and Gottstein and Shvindlerman (1999).

A2.7.2.1 Measurements of individual boundaries

- **Curvature or capillary induced migration**

Many early measurements of boundary mobility were made on bicrystals, where the boundary is driven by the shape of the sample, such as a wedge bicrystal (e.g. fig. 5.4). More recently, Shvindlerman and colleagues have made extensive use of an x-ray tracking method to measure boundary velocities dynamically under a constant driving pressure provided by the boundary curvature in a bicrystal (e.g. Gottstein and Shvindlerman 1999). The sample is oriented so that diffraction is obtained from one grain, and a detector monitors the diffracted intensity at the boundary, the sample being automatically moved so as to maintain a constant diffracted intensity. The sample velocity is thus equal to the boundary velocity, and the method has the advantage that the driving pressure remains constant. Several examples of the results of this type of experiment are given in chapter 5, e.g. figures 5.9 and 5.12.

These experiments are very suitable for obtaining fundamental information about the migration of specific types of boundary, and can be used to investigate the effects of small orientation changes or solute additions. The main disadvantage is that the driving pressures are low, and therefore experiments cannot be carried out on very low angle boundaries nor at low temperatures. The boundary migration occurs under grain growth conditions and it is not yet clear if the boundary behaviour is identical to that during recrystallization.

- **Defect induced migration**

The migration of individual recrystallizing boundaries in single crystals which have either been deformed to produce a substructure, or which have lineage structure formed

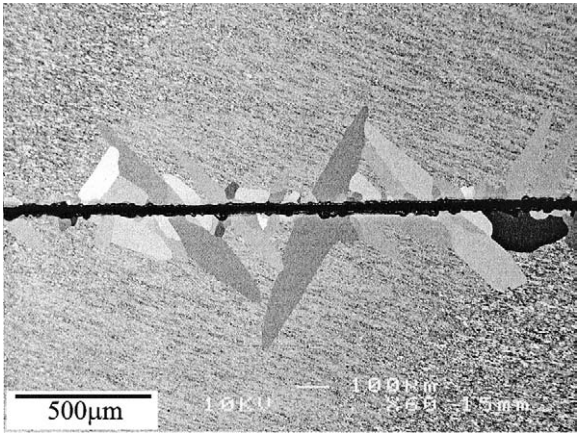

Fig. A2.2. SEM backscattered electron image from an in-situ annealing experiment to determine the growth rate of grains nucleated at the horizontal scratch, and growing into the recovered matrix, (Huang and Humphreys 1999b).

during solidification, has been extensively studied. The well known experiments of Liebmann et al. (1956) on the orientation dependence of mobility were made on deformed single crystals, and those of Aust and Rutter (1959a,b), on the effect of impurities on mobility (fig. 5.21) were made on crystals containing lineage substructures.

Huang and Humphreys (1999a) used a related technique for in-situ SEM measurements of boundary migration in deformed single crystals. The crystal was scratched to provide nucleation sites for the recrystallization which occurred on heating the sample (fig. A2.2). EBSD was used to measure the subgrain sizes and misorientations in the recovered crystals, so that the driving pressure could be calculated (equation 2.8) and also to determine the orientations of the recrystallizing grains and the recovered matrix. The variation of mobility with misorientation obtained in this way is shown in figure 5.11.

Although experiments in which boundaries migrate into a deformed or recovered substructure do not provide the detailed physical insight that can be provided by the curvature driven experiments, they provide valuable data relevant to the recrystallization of metals and can provide the required input for annealing models.

A2.7.2.2 Mean values from subgrain or grain assemblies

Many experiments in which the growth rates of polycrystalline assemblies have been measured have been carried out. If these can be analysed correctly, they provide mean values of the boundary mobility. However, as discussed in §11.1.4, many of these experiments do not obey the simple growth law of equation 11.5, and therefore analysis is difficult. It is likely that in many cases the samples are not 'ideal' because of the presence of second-phase particles or textures.

Measurements of the growth of subgrain assemblies in which the range of misorientations is small, have been made by Huang and Humphreys (2000) (figs. 5.5 and 5.6). Although these only provide mean values, the method is one of the few available for obtaining the mobilities of low angle boundaries.

The project by Rollett and colleagues in which the geometry of triple junctions was measured (see A2.7.1), has also provided information about boundary mobilities (e.g. Yang et al. 2001). Results to date indicate a similar effect of misorientation on mobility to that shown in figures 5.5 and 5.6.

A2.8 PARAMETERS OF TWO-PHASE ALLOYS

In order to quantify the annealing behaviour of two-phase alloys, it is necessary to define the various parameters which describe a distribution of second-phase particles. Experimental measurements are carried out using standard methods of optical, scanning or transmission electron microscopy as appropriate and will not be discussed further. From such measurements a number of parameters may be obtained, and in the following sections we consider only the simplest cases; for more detailed discussion the reader is referred to Underwood (1970), Exner (1972) or Martin (1980).

A2.8.1 Particle size

All multi-phase materials contain particles of a spectrum of sizes and shapes. In modelling the effect of particles it is often necessary to simplify the situation and to assume that the dispersion is of uniform spheres of radius **r.** In comparing experimental data with such a model, a mean value of particle diameter is often used, and for the case of non-spherical but equiaxed particles, an equivalent radius is usually calculated. For particles which are not equiaxed, it is necessary to use more than one parameter to define the particle size and shape.

A2.8.2 Volume fraction

The volume fraction F_V of particles may be measured experimentally or calculated from a knowledge of the phase diagram. For a random distribution of particles, F_V is also equal to the fractional area occupied by particles on a plane section, and the fractional length occupied by the particles on a random straight line.

A2.8.3 Interparticle spacing

For a dispersion of uniform spheres of radius **r,** the **number of particles per unit volume** (N_V) is related to the volume fraction by

$$N_V = \frac{3F_V}{4\pi r^3} \tag{A2.11}$$

The **number of particles intersecting unit area** (N_S) of a plane surface is $N_V.2r$ and hence

$$N_S = \frac{3F_V}{2\pi r^2} \tag{A2.12}$$

If the particles are arranged on a square lattice, then the centre to centre **nearest neighbour spacing on a plane** is

$$\lambda = N_S^{-1/2} \tag{A2.13}$$

For randomly distributed particles, the centre to centre **nearest neighbour spacing on a plane** is

$$\Delta_2 = 0.5N_S^{-1/2} \tag{A2.14}$$

and the centre to centre **nearest neighbour spacing in the volume** is

$$\Delta_3 = 0.554N_V^{-1/3} \tag{A2.15}$$

A2.8.4 Particle distribution

The spatial distribution of the particles, i.e. whether it is uniform, random or clustered may be important. However, there is as yet no simple method of quantitative classification (Fridy et al. 1992).